ACS Macro Letters

Letter

pubs.acs.org/macroletters

Ultrafine Cellulose Nanofibers as Efficient Adsorbents for Removal of UO_2^{2+} in Water

Hongyang Ma, Benjamin S. Hsiao,* and Benjamin Chu*

Department of Chemistry, Stony Brook University, Stony Brook, New York 11794-3400, United States

ABSTRACT: Ultrafine cellulose nanofibers, 5−10 nm in diameter, were prepared from oxidation of wood pulp using the (2,2,6,6-tetramethylpiperidin-1-yl)oxyl (TEMPO)/NaBr/NaClO process followed by mechanical treatment. Carboxylate groups on the surface of these nanofibers provide negative charges, which are very effective to adsorb radioactive UO_2^{2+} in water, evidenced by static adsorption and high resolution transmission electron microscopy (TEM) measurements. The UO_2^{2+} adsorption capability of ultrafine cellulose nanofibers was about 167 mg/g, which is 2−3 times higher than those of typical adsorbents such as montmorillonite, ion imprinted polymer particles, modified silica particles/fibrous membranes, and hydrogels. The high UO_2^{2+} adsorption capability can be attributed to the very high surface-to-volume ratio, high surface charge density, and hydrophilicity of ultrafine cellulose nanofibers, which can be used as effective media to remove radioactive metals from radio-nuclear wastewater.

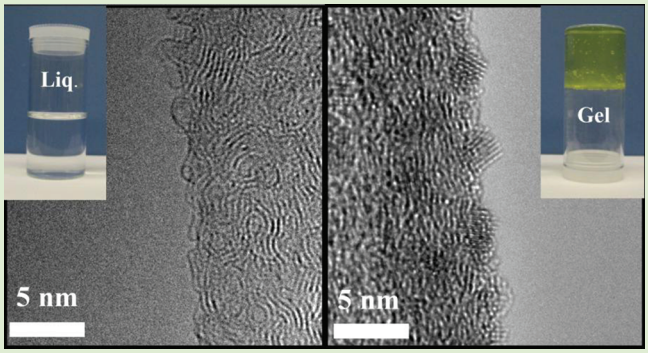

The survival of mankind will face many challenges in the future. One of the challenges is water pollution, as more and more water sources (e.g., oceans, rivers, and lakes) are becoming polluted by different kinds of contaminants, including radioactive species (e.g., U^{238}, Cs^{137}, Pu^{239}, and I^{131}) accidentally discharged during nuclear power plant catastrophies.[1,2] The new and more efficient cleaning technology (e.g., highly efficient adsorbents) to treat radioactive nuclear wastewater has thus become particularly urgent.[3−6] Currently, there are several types of materials that can be used to remove uranyl ions (UO_2^{2+}) in water. For example, clay (montmorillonite, kaolinite) can be used to adsorb UO_2^{2+} through ion-exchange, where its adsorption capacity is in the range of 54.0−98.0 mg/g of clay.[7] Another type of adsorbent is based on the coordination of special ligands and uranyl ion. Ion imprinted polymers containing such adsorbents have shown the maximum UO_2^{2+} adsorption capacity of 98.5 mg/g.[8,9] Chemically modified silica particles[10−12] infused in polyethylene fibrous membranes[13] have also shown decent UO_2^{2+} adsorption capacity, ranging from 10.0 to 47.0 mg/g particle. Hydrogels prepared from appropriate copolymers are efficient adsorbents with the UO_2^{2+} adsorption capacity of 22−156 mg/g dry gel, depending on the charge interaction and diffusion pathways. However, the adsorption of UO_2^{2+} in hydrogel can take a long time to reach equilibrium.[14] Finally, other radioactive contaminants, such as transuranium elements (e.g., plutonium americium, curium, and neptunium), can also be removed via ion-exchange[15−17] and complex physical-chemical processes; these contaminants are usually unstable and decay radioactively, forming other elements.[18]

Ultrafine cellulose nanofibers are unique nanoscaled materials fabricated from wood, cotton, or crustaceans through oxidation via TEMPO/NaBr/NaClO reaction and subsequent mechanical treatment.[19−22] The ultrafine cellulose nanofibers possess very small fiber diameters in the range of a few nanometers (e.g., 5−20 nm) and fiber length in micrometers (e.g., 1−100 μm), depending on the cellulose source. These fibers achieve remarkably high surface-to-volume ratios.[10] Large amounts of ionic hydroxyl, carboxylate, and aldehyde groups are present on the surface of these ultrafine cellulose nanofibers, generated by the oxidation of C6-hydroxyl groups that also enable the stabilization of nanofiber suspension in water.[23] It has been demonstrated that the carboxylate groups, having negative charges, could serve as adsorption sites for positively charged species, such as dyes,[24] viruses,[22-24] and heavy metal ions. By taking advantage of this characteristic in oxidized ultrafine cellulose nanofibers, we demonstrate that these nanofibers can be used as effective media to remove radioactive ions, for example, UO_2^{2+}, with very high adsorption capacity.

An aqueous suspension of 0.05 wt % ultrafine cellulose nanofiber was prepared by the TEMPO/NaBr/NaClO oxidation approach[22] and was used to adsorb UO_2^{2+} from water at pH 6.5 ± 0.5.[25−27] The surface of these cellulose nanofibers was characterized by the conductivity titration measurement.[28,29] The results indicated that the surface contained about 1.4 mmol carboxylate groups per gram of cellulose nanofibers. This value could be considered as the charge density on the surface of nanofibers.[30] The surface morphologies of ultrafine cellulose nanofibers were taken with

Received: September 1, 2011
Accepted: December 9, 2011
Published: December 22, 2011

   dx.doi.org/10.1021/mz200047q | *ACS Macro Lett.* 2012, 1, 213−216

an aberration corrected transmission electron microscope (TEM) operated at 80 kV (FEI Titan 80−300, corrected up to a third-order aberration). To avoid radiation damage of cellulose nanofibers, only 0.1 to 0.5 s of exposure time was used. The representative TEM images of the surface morphologies of ultrafine cellulose nanofibers before and after the UO_2^{2+} adsorption are shown in Figure 1. From

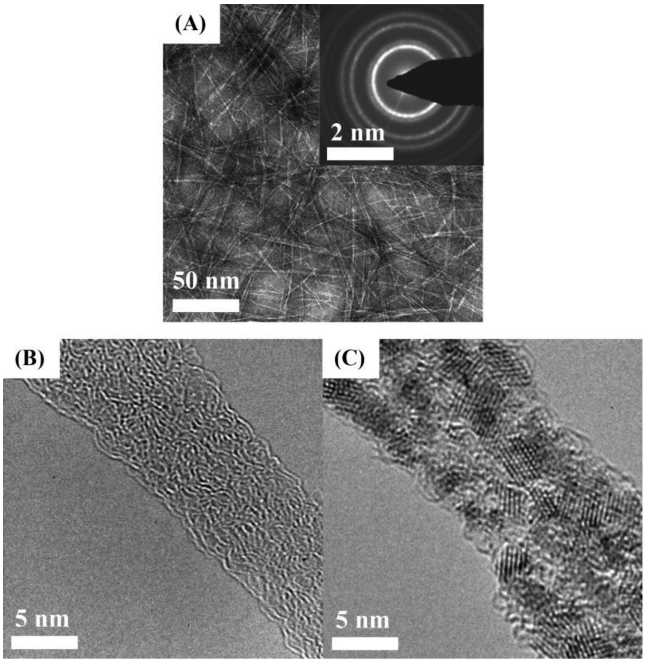

Figure 1. Morphologies of ultrafine cellulose nanofibers, as seen by TEM: (A) typical TEM image of cellulose nanofibers after adsorption of UO_2^{2+}; inset represents the corresponding electron diffraction pattern of cellulose nanofibers; (B) high resolution TEM image of a cellulose nanofiber before the adsorption of UO_2^{2+}; (C) high resolution TEM image of a cellulose nanofiber after the adsorption of UO_2^{2+}.

these images, the diameter of ultrafine cellulose nanofibers was found to be in the range of 5 to 10 nm (Figure 1A, stained with 1.6 wt % of uranyl acetate to distinguish individual fibers in a macroscopic view), and the average aspect ratio of the nanofiber estimated from the TEM image was about 160. The inset in Figure 1A shows a typical electron diffraction pattern of ultrafine cellulose nanofibers, indicating the presence of a type I cellulose crystal form. This observation confirmed that the TEMPO oxidation process primarily occurred on the fiber surface, especially in the amorphous region of cellulose nanofibers.[31] From the high resolution TEM image of Figure 1B (without staining), individual chains of cellulose nanofibers with fingerprint-like configuration were seen.

A total of 1.0 g of uranyl acetate aqueous solution (1.6 wt %) was added to 10 g of cellulose nanofiber suspension (0.05 wt %) under vigorous stirring. The pH value of the mixture was 6.5 ± 0.5. A gelatin of cellulose nanofiber adsorbed with UO_2^{2+} was observed immediately after mixing and could be collected by filtration using 1.0-μm filter paper (Whatman). The cellulose nanofiber-UO_2^{2+} gel was examined using TEM (Figure 1C). After the UO_2^{2+} adsorption, the surface of cellulose nanofibers became covered with metal ionic crystals, as evidenced by the regular crystal lattice, providing direct proof that the cellulose nanofiber could absorb a high amount of UO_2^{2+}.

To further explore the UO_2^{2+} adsorption capacity of ultrafine cellulose nanofibers, a series of static adsorption experiments was carried out using an aqueous suspension of 0.05 wt % cellulose nanofiber (determined by total organic carbon (TOC) analyzer) at pH 6.5 ± 0.5. Uranyl acetate aqueous solutions with UO_2^{2+} concentrations of 1530, 760, 610, 380, 210, 150, and 80 ppm (determined by UV−vis instrument at 420 nm)[32] were subsequently added into the cellulose nanofiber suspension under vigorous stirring. After 2 h, the gel-like cellulose nanofiber scaffolds adsorbed with UO_2^{2+} were removed by filtering with 1.0 μm filter paper (Whatman) and 0.1 μm PVDF filter (Millipore), separately. It should be clarified that filters with different pore sizes were used to selectively separate the mixture of cellulose nanofibers and uranyl acetate. The 1.0 μm filter could retain the gel-like cellulose nanofibers adsorbed with UO_2^{2+}, while cellulose nanofibers and acetate anions (released from uranyl acetate after adsorption) would pass through the filter. In principle, the TOC results could be used to determine the carbon concentrations contributed by both acetate and cellulose nanofiber components. However, because the 0.1 μm filter allowed acetate anions to pass through the filter while retaining both gel-like cellulose nanofibers adsorbed with UO_2^{2+} and cellulose nanofibers, the TOC results reflected only the concentration of acetate anions released from uranyl acetate after adsorption.

It was found again that a gel was formed immediately upon the addition of UO_2^{2+} ions to the cellulose nanofibers suspension, possibly caused by the coordination between UO_2^{2+} and carboxylate groups located on the surface of ultrafine cellulose nanofibers.[27] In other words, UO_2^{2+} acted as a "cross-linker" to form a nanofibrous aggregate.[11] The FTIR spectra of cellulose nanofibers (Nicolet iS10 FTIR-ATR spectrometer) before and after adsorption of uranyl ions are shown in Figure 2.

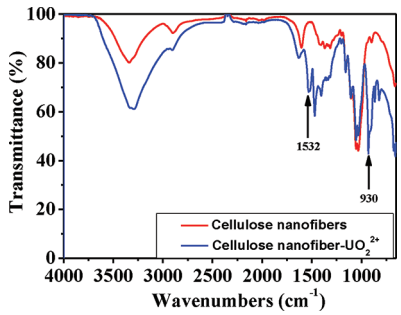

Figure 2. FTIR spectra of cellulose nanofibers before and after UO_2^{2+} adsorption.

It was found that the absorption band associated with carbonyl vibrations at 1604 cm^{-1} in the spectrum of cellulose nanofibers moved to 1634 cm^{-1} after the adsorption of UO_2^{2+} ions. Comparing the spectra of cellulose nanofiber-UO_2^{2+} and cellulose nanofibers, a new asymmetric stretching band at 930 cm^{-1}, which could be assigned to UO_2, and an asymmetric vibration band of the carboxylate groups at 1532 cm^{-1}, were observed in the former. This result confirmed the coordination of the carboxylate groups with UO_2^{2+}.[27,33,34] The threshold concentration of UO_2^{2+} for the formation of the cellulose nanofibrous gel was about 150 ppm, which was determined by

dx.doi.org/10.1021/mz200047q | ACS Macro Lett. 2012, 1, 213−216

the following experiment. When the solution of 80 ppm UO_2^{2+} was added to the cellulose nanofiber suspension, the equilibrium carbon concentration of the filtrate (with 1.0 μm filter) determined by TOC was 140 ppm. This value was due to the combined contributions of cellulose nanofibers and acetate ions of uranyl acetate (the theoretical total carbon concentration is 162 ppm). Therefore, only 22 ppm of carbon, which equals to 50 ppm of cellulose nanofibrous gel, was collected by using a 1.0 μm filter and defined as $c_{cell\text{-}gel}$ in Figure 3. When the

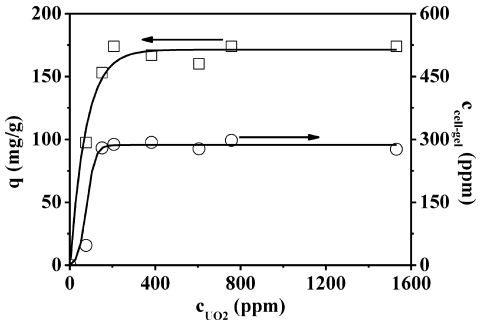

Figure 3. The UO_2^{2+} adsorption capacity (q) and the gel content of ultrafine cellulose nanofibers in suspension as a function of UO_2^{2+} concentration.

UO_2^{2+} solution was higher than 150 ppm, 280 ppm of cellulose nanofibrous gel (i.e., the cellulose nanofiber/UO_2^{2+} aggregate) was formed, which could be removed completely by filtration using a 0.1 μm filter, regardless of the gel formation. The TOC determination of the equilibrium carbon concentration from filtrate was 21 ppm, which was mainly from acetate ions. This result suggests an adsorption mechanism of through coordination between UO_2^{2+} and carboxylate groups located on the surface of cellulose nanofibers, where some excessive acetate ions remained in the equilibrated suspension after filtration. A similar observation was reported in a previous work, where gelation of the 0.2 wt % cellulose nanofiber suspension took place with the increase in ionic strength (created by adding NaCl to >0.008 mol/L).[22] With the increase of UO_2^{2+} concentration to 210 ppm, the amount of cellulose nanofibrous gel ($c_{cell\text{-}gel}$) approached the plateau value of 288 ppm, which remained constant with the increase in the UO_2^{2+}concentration. The adsorption capacity (q_{max}), calculated from the difference between the original and the equilibrium concentration of UO_2^{2+} (determined by UV−vis after filtration with a 0.1 μm filter), was found to be 167 mg/g of cellulose nanofibers. These results exhibited a clear correlation between the content of carboxylate groups of cellulose nanofibers and the UO_2^{2+} adsorption capacity. Furthermore, the content of carboxylate groups distributed on the surface of cellulose nanofibers was 1.4 mmol/g cellulose nanofibers according to the titration measurement. Because the coordination ratio between UO_2^{2+} and carboxylate groups is 1:2,[27] it is expected that 1.0 g of cellulose nanofibers should adsorb 190 mg of UO_2^{2+}. This theoretical value is close to the maximum adsorption capacity of UO_2^{2+} (167 mg/g cellulose nanofiber) determined experimentally. Therefore, the above results confirm that the adsorption mechanism of cellulose nanofibers is mainly based on the coordination of UO_2^{2+} with the carboxylate groups by chelation. The adsorbed UO_2^{2+} could be easily eluted by either nitric acid,[25] hydrochloric acid,[26] sulfuric acid,[27] or Na_2CO_3 solutions,[27] allowing cellulose nanofibers to be recycled.

In summary, it has been shown that ultrafine cellulose nanofibers with negatively charged surfaces containing carboxylate groups can be used to adsorb a radioactive metal ion, UO_2^{2+}. The adsorption capacity of the cellulose nanofiber is very high (167 mg/g of cellulose nanofiber). In addition, the metal ion UO_2^{2+} can serve as a "cross-linker" to aggregate ultrafine cellulose nanofibers and form a gel. The adsorption of UO_2^{2+} on the surface of ultrafine cellulose nanofibers was directly observed by high resolution TEM. Further studies on the adsorption dynamics and infusing cellulose nanofibers into various porous media for practical applications are ongoing in our laboratory.

AUTHOR INFORMATION

Corresponding Author

*E-mail: bhsiao@notes.cc.sunysb.edu (B.S.H.); bchu@notes.cc.sunysb.edu (B.C.).

Notes

The authors declare no competing financial interest.

ACKNOWLEDGMENTS

We thank Prof. Yimei Zhu at Brookhaven National Laboratory (BNL) for taking TEM images. Financial support of this work was provided by the National Science Foundation (DMR-1019370).

REFERENCES

(1) http://www.nytimes.com/2011/03/13/world/asia/13nuclear.html.
(2) http://www.nytimes.com/imagepages/2009/12/17/us/17water_graphic.html.
(3) Fu, F.; Wang, Q. *J. Environ. Manage.* **2011**, *92*, 407−418.
(4) http://www.nrc.gov/reading-rm/doc-collections/nuregs/contract/cr6977/.
(5) Guibal, E. *Sep. Purif. Technol.* **2004**, *38*, 43−74.
(6) Francis, A. J.; Dodge, C. J.; McDonald, J. A; Halada, G. P. *Environ. Sci. Technol.* **2005**, *39*, 5015−5021.
(7) Tsunashima, A.; Brindley, G. W.; Bastovanov, M. *Clays Clay Miner.* **1981**, *29*, 10−16.
(8) Metilda, P.; Gladis, J. M.; Rao, T. P. *Anal. Chim. Acta* **2004**, *512*, 63−73.
(9) Preetha, C. R.; Gladis, J. M.; Rao, T. P. *Environ. Sci. Technol.* **2006**, *40*, 3070−3074.
(10) Jamali, M. R.; Assadi, Y.; Shemirani, F.; Hosseini, M. R. M.; Kozani, R. R.; Farahati, M. M.; Niasari, M. S. *Anal. Chim. Acta* **2006**, *579*, 68−73.
(11) Shamsipur, M.; Fasihi, J.; Ashtari, K. *Anal. Chem.* **2007**, *79*, 7116−7123.
(12) Yousefi, S. R.; Ahmadi, S. J.; Shemirani, F.; Jamali, M. R.; Niasari, M. S. *Talanta* **2009**, *80*, 212−217.
(13) Choi, S. H.; Nho, Y. C. *Appl. Chem.* **1998**, *2*, 668−671.
(14) Caykara, T.; Oren, S.; Kantoglu, O.; Guven, O. *J. Appl. Polym. Sci.* **2000**, *77*, 1037−1043.
(15) Hyde, E. K.; Seaborg, G. T. *The Transuranium Element*, Lawrence Berkeley National Laboratory: University of California, 1956; pp 1−176.
(16) Pages, M.; Clanet, F. *J. Chromotogr.* **1966**, *21*, 105−112.
(17) Haire, R. G.; Young, J. P.; Peterson, J. R.; Benedict, U. *J. Less Common Metals* **1987**, *133*, 167−175.
(18) Schulz, W. W. *The Chemistry of Americium*, Technical Information Center, Energy Research and Development Administration, ERDA Critical Review Series, Atlantic Richfield Hanford Company: Newtown Square, PA, 1976; pp 184−255.
(19) Araki, J.; Wada, M.; Kuga, S. *Langmuir* **2001**, *17*, 21−27.
(20) Saito, T.; Nishiyama, Y.; Putaux, J. L.; Vignon, M.; Isogai, A. *Biomacromolecules* **2007**, *7*, 1687−1691.

(21) Fan, Y. M.; Saito, T.; Isogai, A. *Biomacromolecules* **2008**, *9*, 192−198.
(22) Ma, H. Y.; Burger, C.; Hsiao, B. S.; Chu, B. *Biomacromolecules* **2011**, *12*, 970−976.
(23) Sato, A.; Wang, R.; Ma, H. Y.; Hsiao, B. S.; Chu, B. *J. Electron Microsc.* **2011**, *60*, 201−209.
(24) Ma, H. Y.; Burger, C.; Hsiao, B. S.; Chu, B. *Biomacromolecules* **2011**, DOI: 10.1021/bm201421g.
(25) Jamali, M. R.; Assadi, Y.; Shemirani, F.; Hosseini, M. R. M.; Kozani, R. R.; Masteri-Farahani, M.; Salavati-Niasari, M. S. *Anal. Chim. Acta* **2006**, *579*, 68−73.
(26) Akperov, E. O.; Maharramov, A. M.; Akperov, O. G. *J. Appl. Polym. Sci.* **2010**, *118*, 3570−3575.
(27) Rivas, B. L.; Maturana, H. A.; Peric, I. M.; Pereira, E. *Polym. Bull.* **1996**, *37*, 191−198.
(28) Habibi, Y.; Chanzy, H.; Vignon, M. R. *Cellulose* **2006**, *13*, 679−687.
(29) Saito, T.; Isogai, A. *Biomacromolecules* **2004**, *5*, 1983−1989.
(30) Perez, D. S.; Montanari, S.; Vignon, M. R. *Biomacromolecules* **2003**, *4*, 1417−1425.
(31) Isogai, A.; Saito, T.; Fukuzumi, H. *Nanoscale* **2011**, *3*, 71−85.
(32) Wheeler, J.; Thomas, J. K. *J. Phys. Chem.* **1984**, *88*, 750−754.
(33) Azhgozhinova, G. S.; Guven, O.; Pekel, N.; Dubolazov, A. V.; Mun, G. A.; Nurkeeva, Z. S. *J. Colloid Interface Sci.* **2004**, *278*, 155−159.
(34) Kakihana, M.; Nagumo, T.; Okamoto, M; Kakihana, H. *J. Phys. Chem.* **1987**, *91*, 6128−6136.